Heliyon 10 (2024) e25601

Contents lists available at ScienceDirect

Heliyon

journal homepage: www.cell.com/heliyon

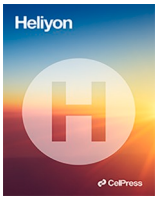

Research article

Garcinone C attenuates RANKL-induced osteoclast differentiation and oxidative stress by activating Nrf2/HO-1 and inhibiting the NF-kB signaling pathway

Hongyun Ji [a,1], Qian Pan [a,1], Ruihong Cao [a,1], Yajun Li [a,b], Yunshang Yang [a,b], Shuangshuang Chen [a], Yong Gu [a,b], Daoyi Qian [a,b], Yang Guo [c], Liangliang Wang [d,**], Zhirong Wang [a,b,***], Long Xiao [a,b,*]

[a] *Translational Medical Innovation Center, Zhangjiagang TCM Hospital Affiliated to Nanjing University of Chinese Medicine, Zhangjiagang, 215600, China*

[b] *Department of Orthopedics, Zhangjiagang TCM Hospital Affiliated to Nanjing University of Chinese Medicine, Zhangjiagang, 215600, China*

[c] *Laboratory of New Techniques of Restoration & Reconstruction of Orthopedics and Traumatology, Nanjing University of Chinese Medicine, Nanjing, 210000, China*

[d] *Department of Orthopedics, The Affiliated Changzhou Second People's Hospital of Nanjing Medical University, Changzhou, 213000, China*

ARTICLE INFO

Keywords:
Osteoporosis
Garcinone C
Reactive oxygen species
NF-κB
Osteoclast

ABSTRACT

Osteoporosis is the result of osteoclast formation exceeding osteoblast production, and current osteoporosis treatments targeting excessive osteoclast bone resorption have serious adverse effects. There is a need to fully understand the mechanisms of osteoclast-mediated bone resorption, identify new drug targets, and find better drugs to treat osteoporosis. Gar C (Gar C) is a major naturally occurring phytochemical isolated from mangosteen, and is a derivative of the naturally occurring phenolic antioxidant lutein. We used an OP mouse model established by ovariectomy (OVX). We found that treatment with Gar C significantly increased bone mineral density and significantly decreased the expression of TRAP, NFATC1 and CTSK relative to untreated OP mice. We found that Garcinone C could disrupt osteoclast activation and resorption functions by inhibiting RANKL-induced osteoclast differentiation as well as inhibiting the formation of multinucleated osteoclasts. Immunoblotting showed that Gar C downregulated the expression of osteoclast-related proteins. In addition, Gar C significantly inhibited RANKL-induced ROS production and affected NF-κB activity by inhibiting phosphorylation Formylation of P65 and phosphorylation and degradation of ikba. These data suggest that Gar C significantly reduced OVX-induced osteoporosis by inhibiting osteoclastogenesis and oxidative stress in bone tissue. Mechanistically, this effect was associated with inhibition of the ROS-mediated NF-κB pathway.

* Corresponding author. Translational Medical Innovation Center, Zhangjiagang TCM Hospital Affiliated to Nanjing University of Chinese Medicine, Zhangjiagang, 215600, China.

** Corresponding author. Department of Orthopedics, The Affiliated Changzhou Second People's Hospital of Nanjing Medical University, Changzhou, 213000, China.

*** Corresponding author. Translational Medical Innovation Center, Zhangjiagang TCM Hospital Affiliated to Nanjing University of Chinese Medicine, Zhangjiagang, 215600, China.

E-mail addresses: 18862238837@163.com (L. Wang), zjgfy_spine_wzr@njucm.edu.cn (Z. Wang), zjgfy_spine_xl@njucm.edu.cn (L. Xiao).

[1] First authors with equal contribution.

https://doi.org/10.1016/j.heliyon.2024.e25601
Received 2 October 2023; Received in revised form 30 January 2024; Accepted 30 January 2024
Available online 1 February 2024

1. Introduction

Osteoporosis is a common bone metabolism disease characterized by low bone mass and the deterioration of bone tissue microarchitecture, which increases the risk of bone fragility and fracture and is recognized as a serious public health problem worldwide. It is estimated that more than 200 million people currently suffer from osteoporosis, and the number of people affected is increasing dramatically due to an aging population and longer life expectancy [1]. Osteoporosis usually occurs in postmenopausal women and the elderly population [2,3]. Drugs that are used clinically to treat osteoporosis include antiresorptive bisphosphonates, HRT and SERM, as well as anabolic fluorides, anabolic steroids and teriparatide (PTH), all of which have serious drawbacks, including digestive disorders, embolism and cancer [4]. Therefore, the search for better drugs to treat osteoporosis is of great importance in the clinic. Natural products offer a promising alternative therapy for maintaining bone health and preventing metabolic bone disease [4].

Bone remodeling is in a dynamic equilibrium that is maintained by bone formation due to osteoblasts and bone resorption due to osteoclasts [5]. Osteoporosis is the result of osteoclast formation exceeding osteoblast production [6]. Osteoclasts are multinucleated giant cells whose activation process is associated with the cytokines macrophage colony-stimulating factor (M-CSF) and NF-κB ligand receptor activation (RANKL). M-CSF promotes the early proliferation of osteoblasts, and RANKL maintains the function of mature osteoblasts [7]. These two cytokines induce the expression of genes encoding tartrate-resistant acid phosphatase (TRAP) and histone proteinase K (CTSK), which represent the osteoclast spectrum, and TRAP and CTSK degrade bone mineral and collagen matrix, thus mediating bone resorption [8]. Current osteoporosis therapies targeting excessive bone resorption have serious adverse effects. Therefore, there is a need to fully understand the mechanisms by which RANKL stimulates osteoclast-mediated bone resorption to identify new drug targets and find better therapeutic approaches [9].

Reactive oxygen species (ROS) can accelerate bone resorption through osteoclast dysfunction [10]. ROS are potent and multifunctional signaling molecules that influence various pathways of osteoclast differentiation. Excess superoxide anion radical (O2-) and the redox radical H2O2 promote osteoclast activity, affect their differentiation and prolong the lifespan of mature osteoclasts through an inflammation-induced cascade response [10]. There is growing evidence of the importance of ROS in osteoclasts, and an increase in ROS due to aging or increased inflammation stimulates bone resorption and exacerbates bone loss [11].

Garcinone C (Gar C), which is the main natural phytochemical isolated from the fruit mangosteen, also possesses good antioxidant activity and is a derivative of the natural phenolic antioxidant lutein [12]. Mangosteen is known for its antioxidant [13,14], anti-inflammatory [15] and anticancer activities [16–18]. Gar C has recently been reported to have protective effects against rectal, colon and nasopharyngeal cancers [18–20]. Indeed, antitumor activity is closely related to antioxidant activity. Carcinogenesis is to a great extent due to ROS-induced oxidative damage. Although there have been some reports on the biological activity of Gar C, the role of Gar C as a potential agent affecting osteoclast formation has not yet been clearly demonstrated. Therefore, in the present study, we investigated the therapeutic effects of Gar C on osteoporosis. The mechanism by which Gar C inhibits osteoclast differentiation was further examined.

2. Experiments

2.1. Pharmacological intervention in the ovariectomy (OVX)-induced osteoporosis mouse model

AEWC approval was obtained (approval date: 2022-04-12, approval number: AEWC- 20220412). The mice were randomly divided into 4 groups: sham-operated, OVX, OVX + low-dose Gar C (5 mg/kg), and OVX + high-dose Gar C (25 mg/kg).We constructed a mouse model of OVX-induced osteoporosis. In the OVX group and the OVX + Gar C group, respectively, an incision of about 1.5 cm in length was made in the middle of the lower abdomen of the mice under anesthesia and the incision was sutured after removing the bilateral ovaries and the surrounding adipose tissue. In the Sham group, only the ovaries were exposed, and the surrounding adipose tissue was removed and then incorporated into the abdominal suture to close the incision [21].The JONN laboratory in Suzhou, China, provided us with 24 experimental C57BL/6 mice (no. 202236274). These mice were 6 weeks old and weighed 20 g on average. After 3

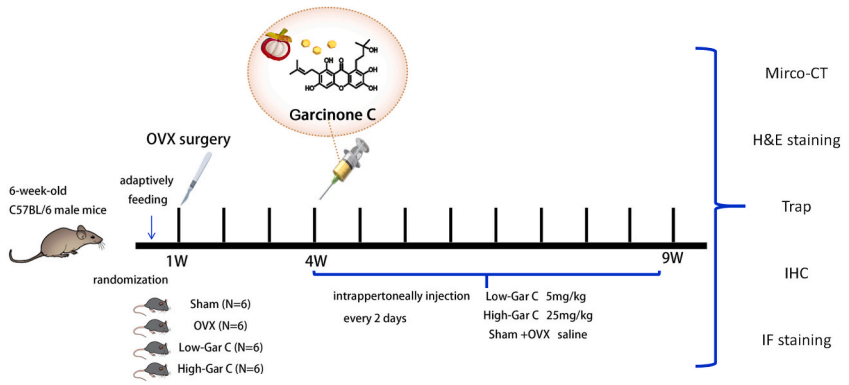

Fig. 1. Schematic diagram of the animal experimental design.

weeks, 5 mg/kg Gar C was injected intraperitoneally every 2 days in the OVX + Gar C low-dose group, and 25 mg/kg Gar C was injected intraperitoneally every 2 days in the OVX + Gar C high-dose group, Mice in the sham-operated and OVX groups were injected with the same amount of normal saline [21,22].After 8 weeks, the femur and spine were removed and fixed in 4 % paraformaldehyde (Fig. 1).

2.2. Micro-CT (μCT) bone histomorphometric analysis

The left femur of each mouse was carefully stripped of the ligaments, muscles and other soft tissues, and the cleaned femur was fixed in 4 % paraformaldehyde for 3 d and then transferred to a labeled 15 ml centrifuge tube filled with saline for storage in preparation for the μCT scan. The following μCT scan data were collected: bone density parameters (BMD), bone surface area (BS), bone volume (BV), the ratio of trabeculae to total bone tissue volume (BV/TV), the bone surface area to tissue volume ratio (BS/TV), the number of trabeculae (Tb.N) and trabecular separation (Tb.Sp). The 3D images of the spine were reconstructed using the μCT 3D reconstruction software, and the relevant parameters were analyzed.

2.3. Hematoxylin-eosin (H&E) staining and TRAP staining of the right femur

The soft tissue incidental to the right femur was stripped, each femur was labeled, and the femur was fixed and then decalcified. After these procedures were completed, the specimens were sectioned, and the histological structure of the distal femur was analyzed by H&E and TRAP staining. After being stained, the tissue sections were preserved and observed using an inverted phase contrast microscope, and the appropriate areas were selected and photographed for preservation and analysis.

2.4. Immunohistochemical analysis

We dewaxed and rehydrated the sections, which were then incubated with primary antibodies against CTSK (GB11276, Servicebio, Wuhan, China) and NFATC1 (GB111027, Servicebio, Wuhan, China). After 12 h, the sections were washed and incubated with the appropriate secondary antibody for 30 min. The stained sections were photographed using a Nikon Eclipse CiL light microscope (Nikon, Tokyo, Japan).

2.5. Fluorescent double staining

The sections were fixed with 4 % paraformaldehyde and labeled with MMP9 (GB12132, Servicebio, Wuhan, China),NFATC1 (GB111027, Servicebio, Wuhan, China), CTSK(GB111276, Servicebio, Wuhan, China), Nrf2(GB113808, Servicebio, Wuhan, China) and HO-1 (GB11104, Servicebio, Wuhan, China) antibodies. The primary antibodies were rinsed in PBS and then rinsed in Triton X-100 for 10 min. Normal sheep serum was added and incubated for 30 min. The primary antibody was incubated in rabbit anti-GFAP (Beijing ZhongShan) incubation solution for 1 h and left overnight at room temperature. The sections were rinsed with PBS and then incubated with FITC-labeled goat anti-rabbit G (Beijing Zhongxuan) fluorescent secondary antibodies for 1 h. The sections were washed well with PBS. After being washed with PBS, Cy3-labeled goat anti-mouse (Beijing Zhongsugi) fluorescent secondary antibodies were added and incubated for 1 h at room temperature. The sections were then washed with PBS. The samples were observed by fluorescence confocal microscopy.

2.6. Cell culture

RAW264.7 cells (FH0328, FuHeng BioLogy, Shanghai, China) were cultured in 10 % fetal bovine serum and 100 μ/mL penicillin–streptomycin-amphotericin B in DMEM and passaged for growth and drug intervention, and the medium was changed every other day.

BMDM were obtained from the fresh femurs of 6-week-old C57/BL6 mice and cultured in medium containing 10 % fetal bovine serum, 50 ng/mL M-CSF and 100 μ/mL penicillin-streptomycin-amphotericin B in AMEM.

2.7. Cytotoxicity assay

The cytotoxicity of Gar C (HY–N6954, MCE, New Jersey, USA) was measured by the CCK-8 method. RAW264.7 or BMDM were seeded in 96-well plates at $1*10^4$/well, incubated for 3–4 h and then treated with different concentrations of Gar C (0, 0.05, 0.5, 5 and 50 μmol/L) for 1, 2 and 3 d. Interventions were performed for 1, 2 and 3 d, followed by the addition of 10 μl of CCK-8 buffer and incubation at 37 °C, after which the absorbance at 450 nm was measured using an enzyme marker (BioTek, Vermont, USA).

2.8. TRAP staining

BMDM or RAW264.7 cells (5×10^4/well) were inoculated in 12-well plates, incubated with 50 ng/mL M-CSF and 50 ng/ml RANKL, and then treated with 0, 0.2, 1, and 5 μmol/L Gar C for 5 d. The cells were stained using the TRAP staining kit (387A-1 KT, Sigma) and photographed. The mean area of osteoclasts per well was measured using ImageJ software (NIH, Bethesda, Maryland, USA).

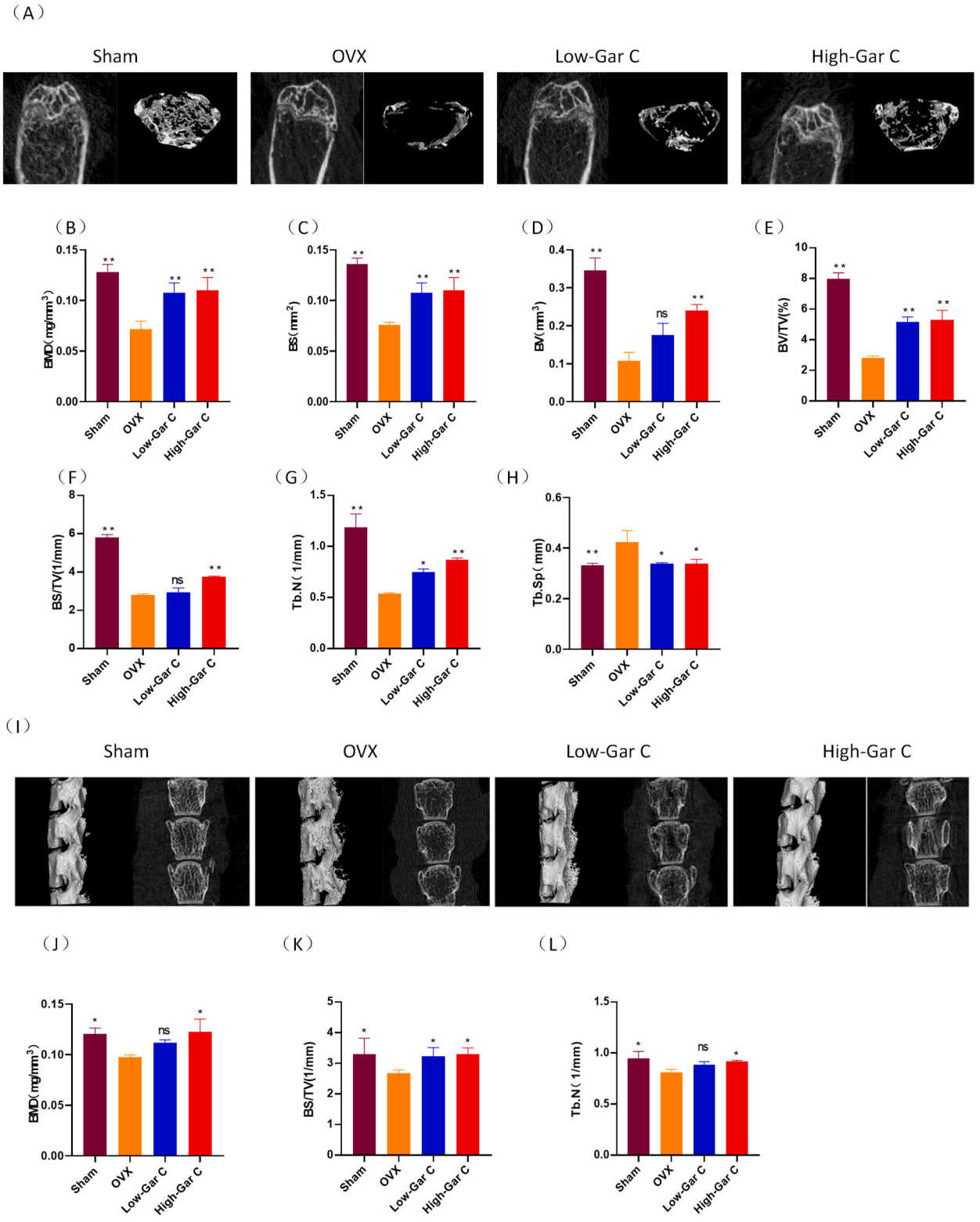

Fig. 2. Gar C attenuates bone loss in OVX model mice. (A) Representative 3D-CT images of the femur in each group. (B–H) Statistical analysis of structural parameters of the distal femur.(I) Representative 3D-CT images of the spine in each group. (J–L) Statistical analysis of structural parameters of the spine. Note: * indicates $P < 0.05$, ** indicates $P < 0.01$ (relative to the OVX group).

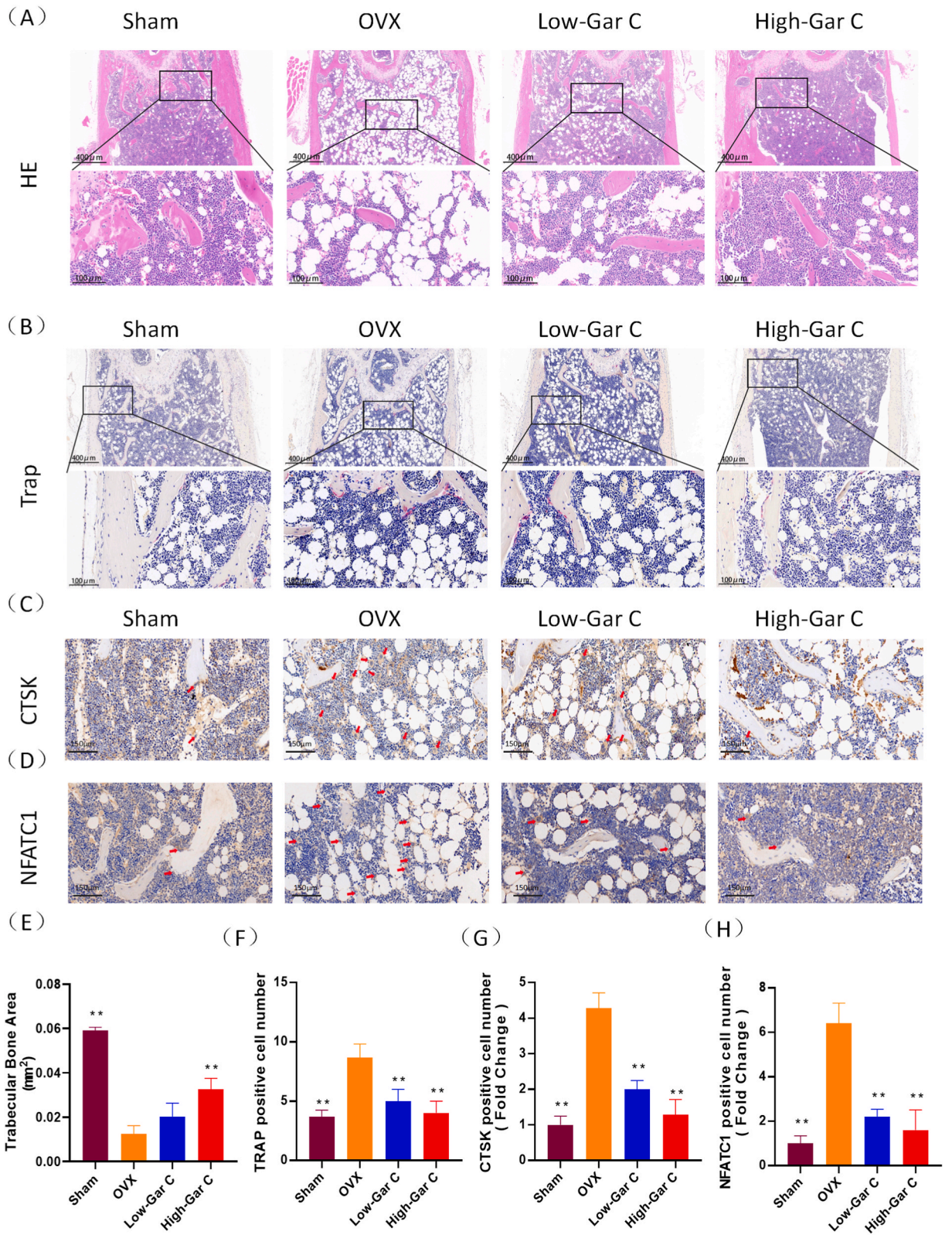

(caption on next page)

Fig. 3. Reduced bone loss in OVX mice treated with Gar C. (A) H&E staining of femoral sections from each group of mice (scale bar = 100 μm). (B) TRAP activity in femoral sections from each group of mice (scale bar = 100 μm). (C–D) Osteoclast-associated IHC staining: CTSK and NFATC1 (scale bar = 150 μm). (E) Quantification of the trabecular bone area in femoral sections from each group of mice. (F) Quantitative analysis of the number of TRAP-positive cells in the femoral sections of mice in each group. (G–H) Quantitative analysis of IHC staining: CTSK and NFATC1. Note: * indicates $P < 0.05$, ** represents $P < 0.01$ (relative to the OVX group).

2.9. Immunofluorescence staining

RAW264.7 cells were inoculated into 24-well plates and incubated until they formed mature osteoclasts in response to stimulation with M-CSF and RANKL. Gar C (0, 0.2, 1, 5 μmol/L) was added to the medium for 5 d, followed by incubation with the molecular probe Alexa Fluor 488 Phalloidin. The mean area of osteoclasts per well and the number of nuclei were calculated.

2.10. Determination of ROS levels

RAW264.7 cells were pretreated with Gar C (0, 0.2, 1, 5 μmol/L) and 10 μmol/L dichlorodihydrofluorescein (DCFH-DA), shaken and mixed, and incubated for 30 min in a 37 °C incubator protected from light. Relative intracellular ROS levels were observed using fluorescence microscopy, and the FITC fluorescence intensity was measured by flow cytometry.

2.11. Bone plate resorption assay to determine osteoclast function

BMDM (5×10^5 cells) were seeded on sterilized bovine bone slices with a diameter of 12 mm and induced with 50 ng/ml RANKL and 50 ng/mL M-CSF for 10 days while intervening with 0, 0.2, 1, or 5 μM Gar C. At the end, The cells in the bone fragments were lysed with trizol (15596018, Thermo Fisher Scientific, Bothell, WA, USA) for 10 min and then be washed. The area of resorption depression formation on the surface of the bovine bone slices was observed under a scanning electron microscope (Zeiss EVO LS-15).

2.12. Western blot analysis

RAW264.7 cells were treated with Gar C (0, 0.2, 1, 5 μmol/L) for 2 d before total protein was isolated. The protein samples were separated in an electrophoresis apparatus and then transferred to PVDF membranes (microwells), which were blocked and incubated overnight at 4 °C with rabbit primary antibodies. Antibodies against MMP9 (1:1000), CTSK (1:1000), c-Fos (1:1000), NFATC1 (1:1000), HO-1 (1:10000), IκB-α (1:1000), and P65 (1: 1000) were purchased from Abcam (ab38898, ab 19027, ab190289, ab25916, ab68477, ab32518, and ab16502). Antibodies against Nrf2 (1:1000), *p*-IκBα (1:1000), and PP65 (1:1000) were purchased from CST (#33649, #2859, #3031). After being washed with TBST for 15 min, the membranes were incubated with secondary antibodies for 2 h. Finally, the proteins were measured with a chemiluminescent HRP substrate.

2.13. Nrf2 and p65 immunofluorescence staining

RAW264.7 cells were inoculated onto 24-well plates and pretreated with Gar C (5 μM) for 2 h, followed by induction with RANKL (50 ng/ml) for 45 min. The cells were washed three times with PBS, fixed with 4 % paraformaldehyde and permeabilized with 0.1 % Triton X-100. The cells were incubated with rabbit anti–NF–κB p65 and Nrf2 primary antibodies overnight at 4 °C and then probed with Alexa Fluor 488 secondary antibodies in the dark at room temperature for 2 h. The cells were washed in PBS, restained with DAPI for 15 min and observed using fluorescence microscopy.

2.14. Statistical analysis

All experimental data are expressed as the mean ± standard deviation (SD) and were processed using SPSS 25.0 software. Statistical analysis was performed using t tests and analysis of variance (ANOVA). A value of $p < 0.05$ indicated that the differences were statistically significant.

3. Results

3.1. Gar C attenuates bone loss in OVX model mice

μCT analysis of structural parameters of the distal femur in the sham-operated, OVX and OVX + Gar C groups of mice showed that the OVX group exhibited significant bone loss compared to the sham-operated group. Statistical analysis of bone parameters showed an increase in BMD (0.128 ± 0.008 g/cm3 vs. 0.072 ± 0.008 g/cm3) and a decrease in Tb.Sp (0.332 ± 0.007 mm vs. 0.424 ± 0.045 mm) after 8 weeks of Gar C treatment compared to the corresponding values in the OVX group (Fig. 2A,B and H). BS, BV, BV/TV, BS/TV, and Tb.N were elevated, and these parameters were significantly increased in a concentration-dependent manner in the OVX + Gar C group (Fig. 2A,C-G).We also found that Gar C could reduce bone loss in the spine, suggesting that Gar C could reduce bone loss throughout the body (Fig. 2I-L).

After 8 weeks of administration, we observed a significant decrease in BS area in the OVX group compared to the normal group (0.012 ± 0.001 nm^2 vs. 0.059 ± 0.004 nm^2), as observed by morphometric analysis of bone histology by H&E staining, and an increase in BS area in the OVX group + Gar C intervention group with increasing Gar C concentrations (1 μM vs. 5 μM: 0.020 ± 0.006 nm^2 vs. 0.033 ± 0.005 nm^2) (Fig. 3A–E). Similarly, TRAP staining showed that the number of positive cells was significantly higher in the OVX group than in the sham-operated group (8.667 ± 1.155 vs. 3.667 ± 0.577) and that Gar C treatment decreased the number of positive cells per bone surface in a concentration-dependent manner compared to that in the OVX group (1 μM vs. 5 μM: 5.000 ± 1.000 vs. 4.000 ± 1.000) (Fig. 3B–F).

Furthermore, immunohistochemical staining analysis of the osteoclast functional protein CTSK and the associated transcription factor NFATC1 showed that the number of CTSK and NFATC1-positive cells were significantly increased in the OVX group compared to

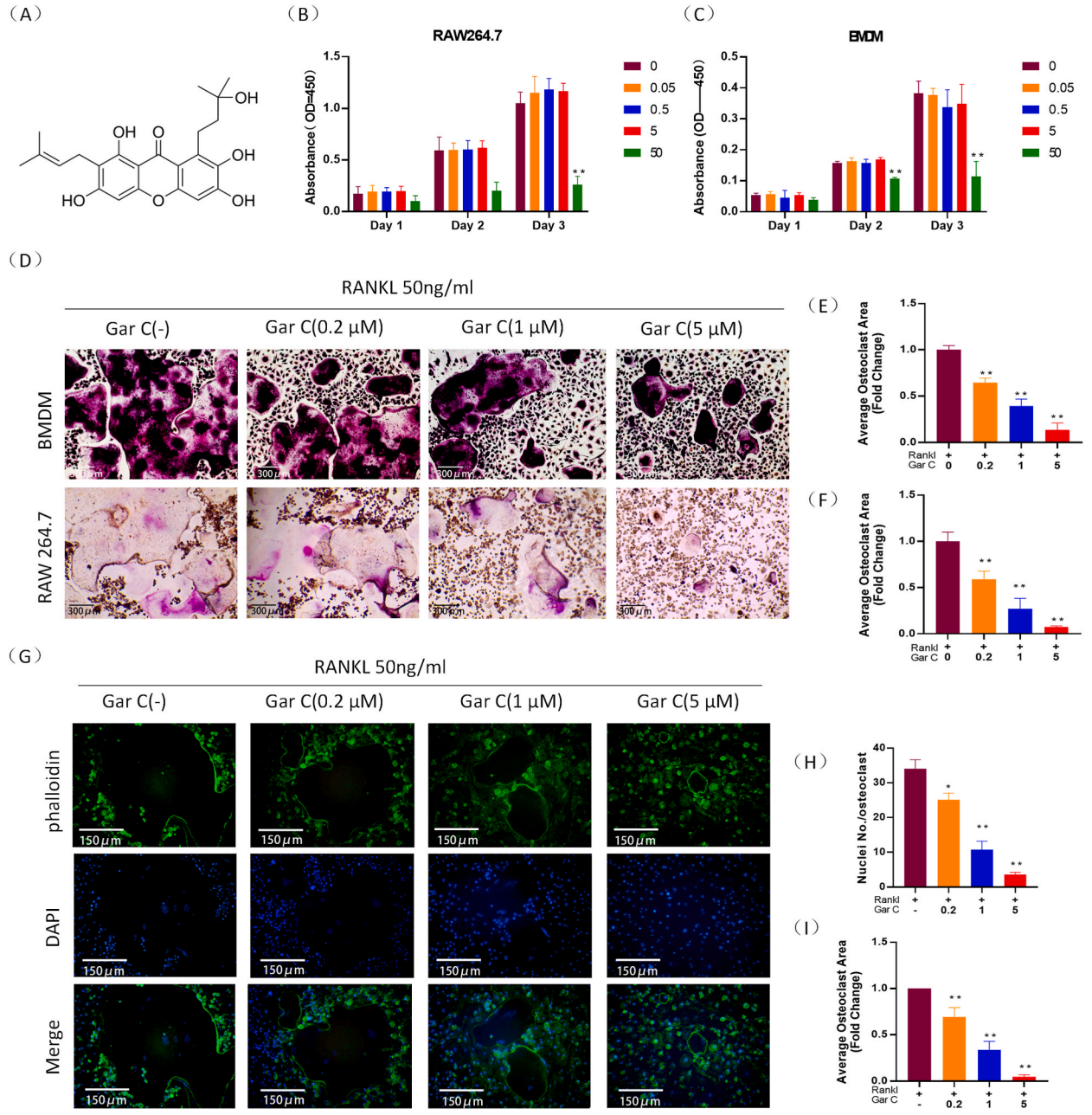

Fig. 4. Gar C inhibits osteoclast differentiation. (A) Molecular formula of Gar C. (B–C) The viability of RAW264.7 cells and BMDM was determined by CCK8 assays. (D) Representative images of TRAP staining (scale bar = 300 μm). (E–F) Quantitative analysis of the osteoclast area in each group. (G) Representative images of actin ring staining (scale bar = 150 μm). (H–I) Quantitative analysis of F-Actin size and the number of nuclei per osteoclast. Note: * indicates $P < 0.05$, ** represents $P < 0.01$.

the sham-operated group, and this effect was improved in the OVX + Gar C group (Fig. 3C–D,G-H).

3.2. Inhibitory effect of Gar C on RANKL-induced osteoclast differentiation

We found that Gar C could reduce the number of TRAP-positive cells during OVX-induced osteoporotic disease progression. To further clarify the effect of Gar C on osteoclast activation, we performed TRAP staining and F-actin ring staining. As determined by CCK8 assays, cell viability was significantly affected when the concentration of Gar C was 50 μM (Fig. 4B and C). Treatment of RAW264.7 cells and BMDMs with 0.05, 0.5 and 5 μM Gar C for 3 d did not affect cell viability but promoted cell proliferation. Based on the CCK8 results (Fig. 4B and C), in subsequent in vitro experiments, 0.2, 1 and 5 μM Gar C were used to treat the cells. To investigate the inhibitory effect of Gar C on RANKL-induced osteoclast differentiation, different concentrations of Gar C (including 0, 0.2, 1 and 5 μM) were administered to RANKL-induced BMDMs and RAW 264.7 cells. TRAP staining showed that Gar C dose-dependently reduced the osteoclast area, and 5 μM induced a significant inhibitory effect (Fig. 4D–F).

The bone resorptive activity of osteoclasts is dependent on their adhesion to the bone surface, and this adhesion correlates with the resorptive function of the osteoclast skeleton closure zone structure, which is the banded F-actin ring, and so we examined mature osteoclasts by assessing the formation of F-actin rings following RANKL stimulation. Osteoclasts were observed by rhodamine ghost pencil staining. The results showed that Gar C significantly inhibited the formation of multinucleated osteoclasts (Fig. 4G–I). Actin rings in the RANKL group showed a large typical ring structure, whereas those in the high Gar C concentration group were significantly smaller.

3.3. Gar C inhibits bone resorption and downregulates osteoclast-associated protein expression

The results of the bone resorption assay are presented that the bone resorption function of osteoclasts was significantly increased

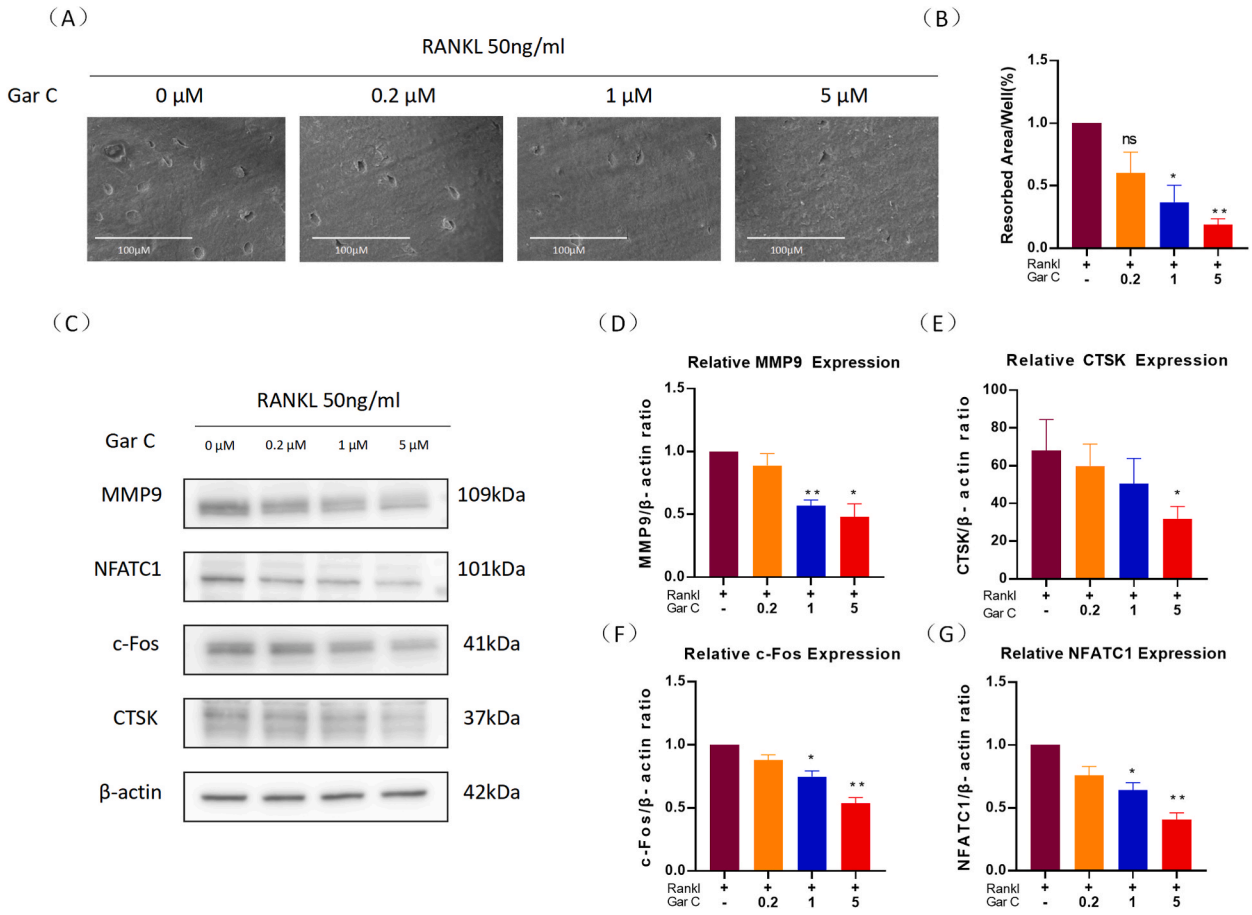

Fig. 5. Gar C inhibits osteoclastic bone resorption activity and The effect of Gar C on RANKL-induced protein of osteoclast-specific MMP9, CTSK c-Fos **and** NFATC1. (A) Representative images of bone resorption. (B) Quantitative analysis of the bone resorption area in each group.(C) Western blot showing MMP9, CTSK, c-Fos, NFATC1 and β-actin. (D–G) Quantitative analysis of the expression of the protein bands relative to β-actin. Note: * indicates $P < 0.05$, ** represents $P < 0.01$.

after RANKL stimulation, but significantly decreased after Gar C treatment (Fig. 5A–B). Quantitative analysis of resorption area showed that Gar C significantly decreased the percentage of bone resorption area in a dose-dependent manner. It showed that Gar C inhibited the in vitro resorption activity of osteoclasts in a dose-dependent manner, demonstrating the anti-bone resorption activity of Gar C. Gar C downregulated the expression of osteoclast-associated proteins. Western blotting showed that the expression of the osteoclast-associated functional proteins MMP9 and CTSK was significantly inhibited in a concentration-dependent manner after Gar C administration (Fig. 5C, D-E). The protein expression of the transcription factors c-Fos and NFATC1, which are associated with osteoclast differentiation, was significantly inhibited by 5 μM Gar C (Fig. 5C, F-G).

3.4. Gar C inhibits RANKL-induced oxidative stress and increases Nrf2 levels

Previous findings confirmed that the level of oxidative stress is increased during osteoclast activation, that ROS play an important role in the differentiation of osteoclasts and that the bone resorption function of osteoclasts is inextricably linked to the stimulation of ROS [23]. Therefore, we further investigated whether Gar C could influence osteoclast activation by affecting the level of oxidative stress. We measured ROS levels during osteoclastogenesis with the dye DCFH-DA to clarify whether Gar C inhibits RANKL-mediated

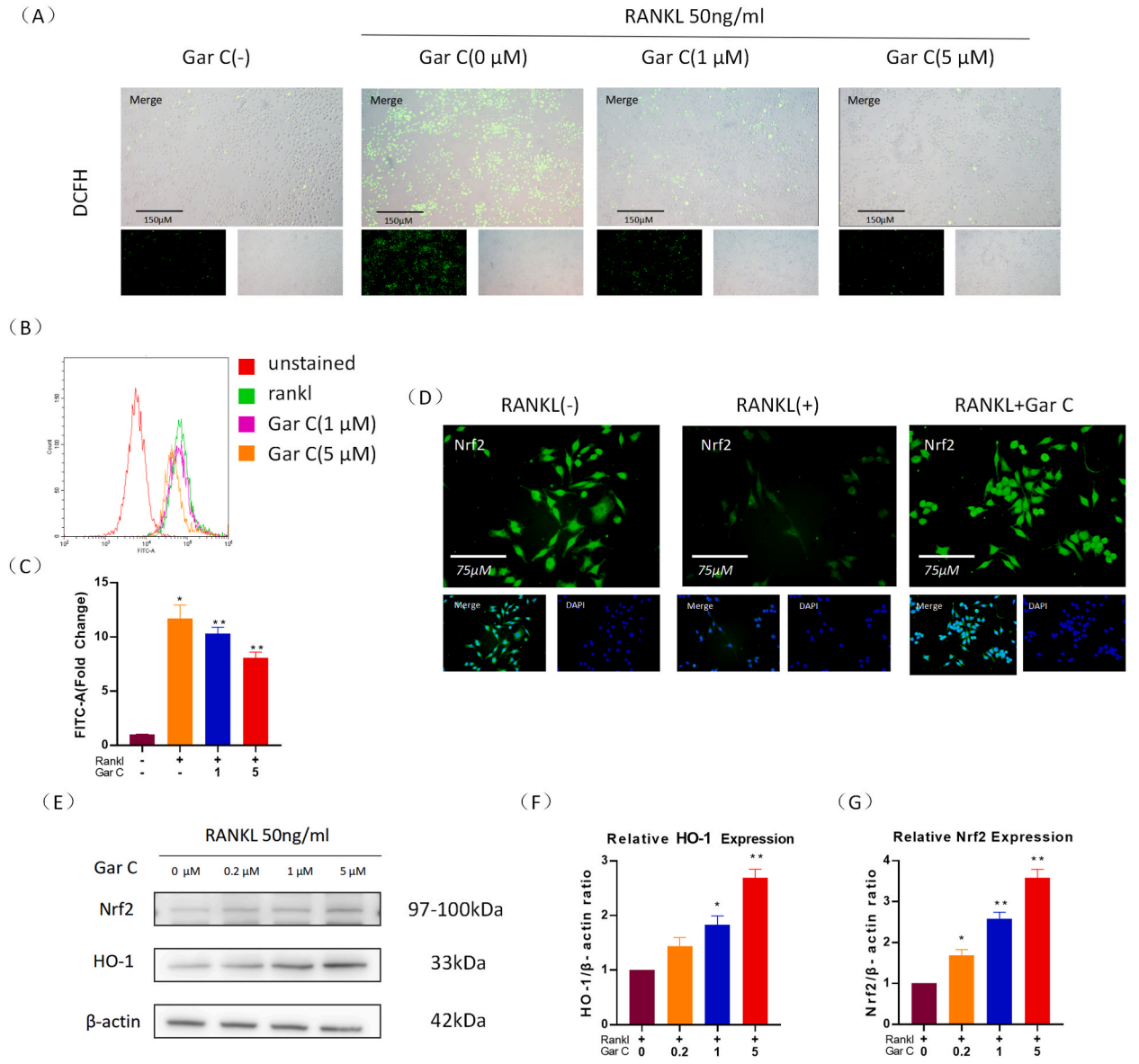

Fig. 6. Gar C reduces RANKL-induced osteoclastogenesis by ROS production. (A) Representative images showing ROS staining (scale bar = 150 μm). (B–C) Flow cytometric analysis of FITC fluorescence intensity and quantitative analysis. (D) Fluorescence intensity of Nrf2 (scale bar = 75 μm). (E) Western blot showing Nrf2 and the antioxidant enzymes HO-1 and β-actin. (F–G) Band intensity of Nrf2 and HO-1 relative to β-actin.

oxidative stress during osteoclastogenesis. We found that RANKL (50 ng/ml) stimulation for 20 min significantly increased ROS levels in RAW264.7 cells, similar to the results of previous studies. Gar C significantly inhibited oxidative stress during RANKL induction (Fig. 6A–C). Immunofluorescence staining showed that Gar C regulates Nrf2 expression in RANKL-stimulated RAW264.7 cells. We found that Gar C pretreatment increased the nuclear translocation of Nrf2 in RANKL-stimulated cells (Fig. 6D). Western blotting

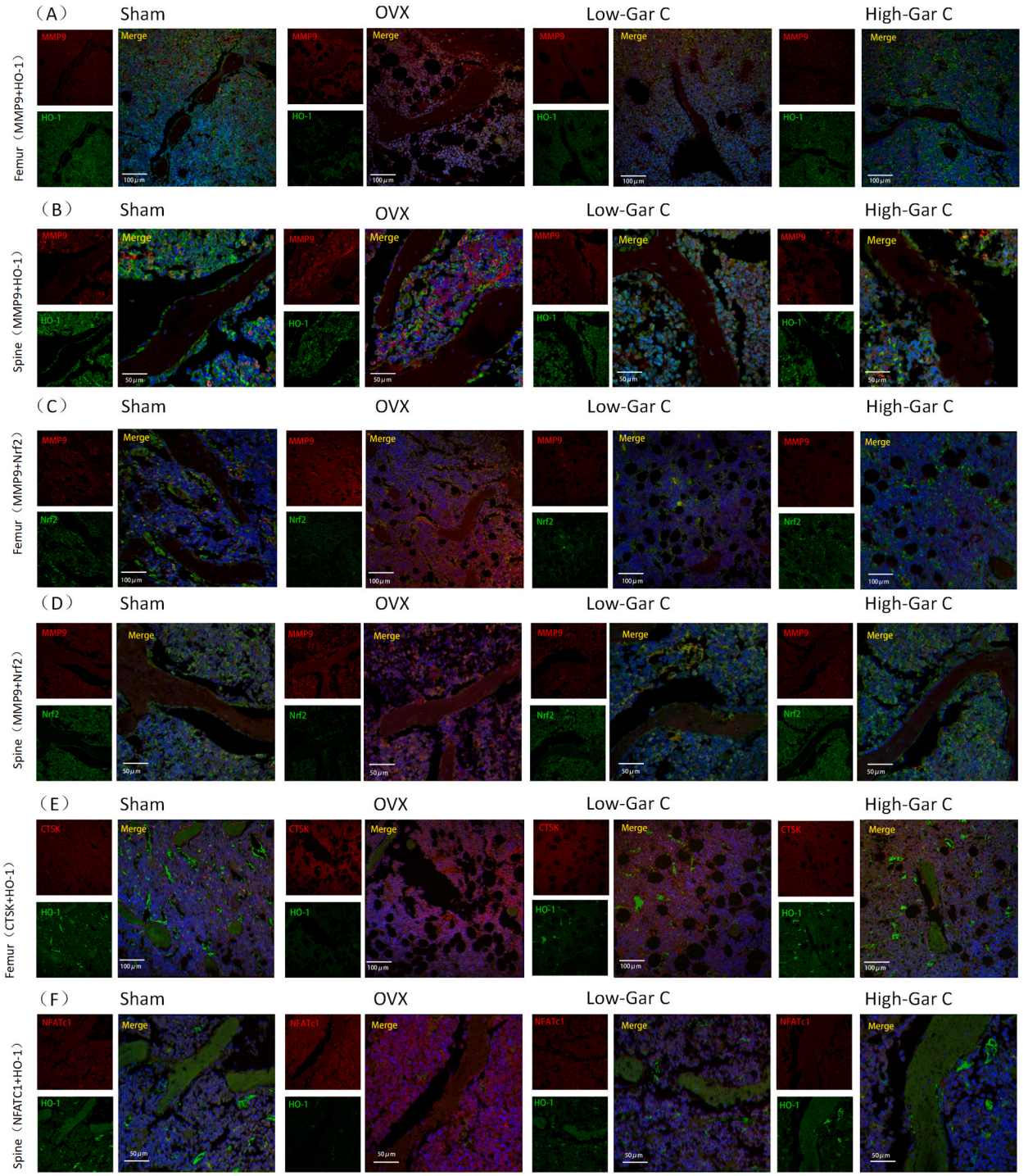

Fig. 7. Gar C enhanced the expression of Nrf2, HO-1 and decreased the expression of MMP9, CTSK and NFATC1 **in vivo.** (A) IHC staining of femoral MMP9+HO-1 (scale bar = 100 μm).(B) IHC staining of spinal MMP9+HO-1 (scale bar = 50 μm) (C)IHC staining of femoral MMP9+Nrf2 (scale bar = 100 μm). (D) IHC staining of spinal MMP9+Nrf2 (scale bar = 50 μm). (E) IHC staining of femoral CTSK + HO-1 (scale bar = 100 μm). (F) IHC staining of spinal NFATC1+HO-1 (scale bar = 50 μm). Note: * indicates $P < 0.05$, ** represents $P < 0.01$.

showed that Gar C significantly increased the expression of Nrf2, a core transcription factor that protects against oxidative stress, and HO-1, a ROS scavenging enzyme (Fig. 6E–G).

Interestingly, in vivo, Nrf2 and HO-1 expression was reduced in the OVX group and increased after Gar C treatment, suggesting that Gar C may inhibit oxidative stress, and the fluorescence staining results showed opposite effects on the expression of Nrf2,HO-1 and the osteoclast-associated protein MMP9,CTSK, NFATC1 further confirming that Gar C is a key player in the regulation of oxidative stress, affects the activation of osteoclasts and attenuates the development of osteoporosis (Fig. 7A–F).

3.5. Gar C inhibits the RANKL-induced NF-κB signaling pathway

ROS can affect the phosphorylation of P65 to regulate NF-κB responses and influence its activation [24]. We have demonstrated that Gar C can affect ROS levels during osteoclastogenesis, and we further investigated the effect of Gar C on the NF-κB signaling

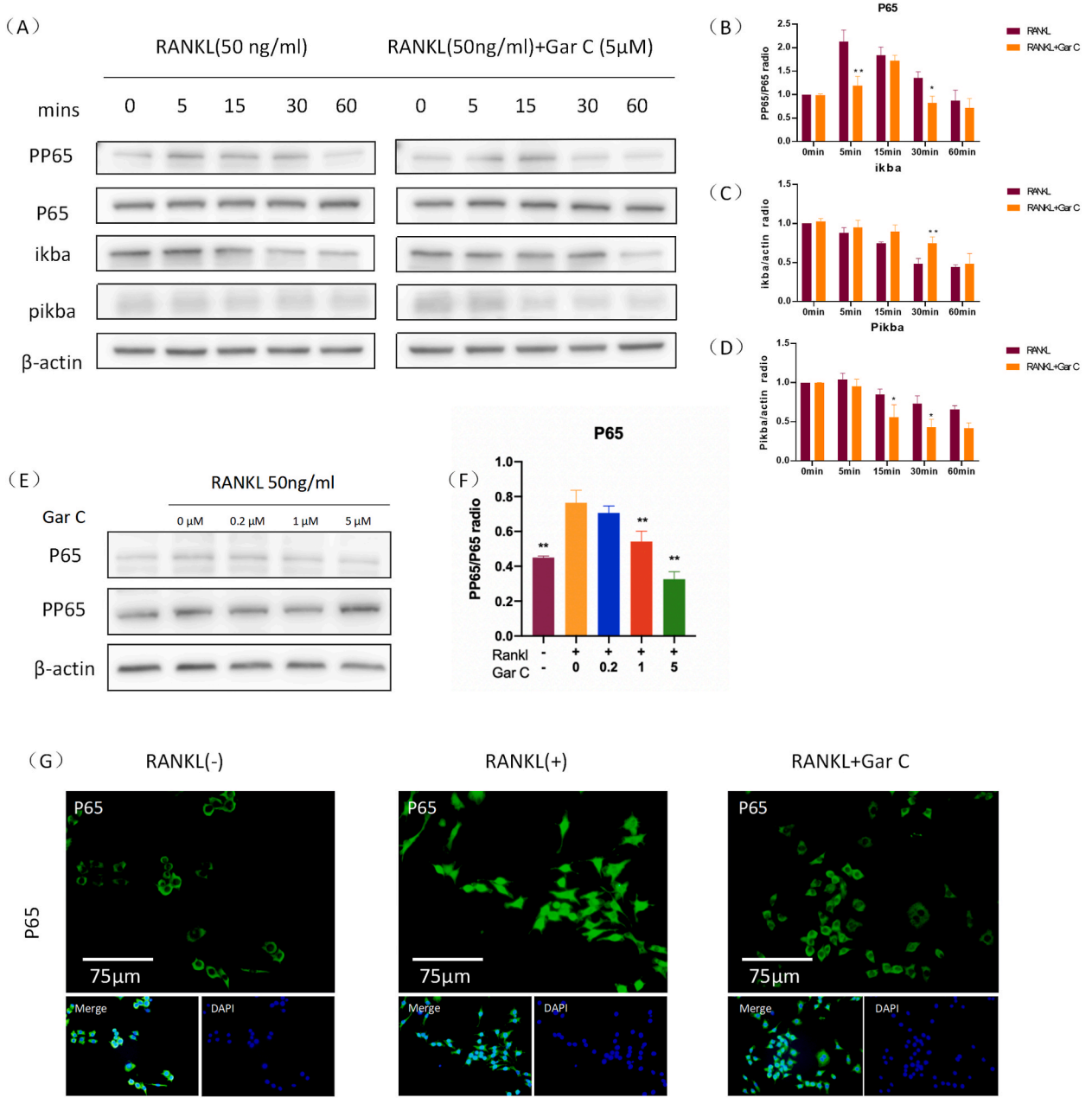

Fig. 8. Gar C inhibits RANKL-induced NF-κB signaling in vitro. (A–F) Western blots showing P65 and IκBα expression and phosphorylation. (G) Immunofluorescence staining of P65 (scale bar = 75 μm). Note: * indicates $P < 0.05$, ** represents $P < 0.01$.

pathway in RAW264.7 cells at different time points. As shown (Fig. 8A–D), the level of phosphorylated P65 (PP65) in the RANKL group increased rapidly after the addition of RANKL and peaked at 5 min, whereas the level of PP65 peaked within 15 min after the addition of RANKL plus Gar C. Gar C delayed the peak of P65 phosphorylation. The level of PP65 was lower in the RANKL + Gar C group than in the RANKL group at the same times. NF-κB activity is regulated by the IκB protein, and we found that Gar C treatment significantly decreased IκBα degradation and phosphorylation at 30 min. Furthermore, the phosphorylation level of P65 decreased with increasing Gar C concentrations after 30 min (Fig. 8E–F). We also detected RANKL-induced nuclear translocation of NF-κB p65 by immunofluorescence analysis (Fig. 8G). We found that Gar C could effectively inhibit the nuclear translocation of p65. These results suggest that Gar C affects oxidative stress levels through the NF-κB pathway.

4. Discussion

Bone is a mature, dynamic but stable connective tissue, and bone remodeling bone formation by osteoblasts and bone resorption by osteoclasts are in equilibrium [25]. Dysregulation of bone homeostasis can lead to a variety of bone diseases, particularly osteoporosis [26]. ROS play an important role in determining the pathogenesis of bone diseases [27]. As intracellular signaling molecules, ROS are regulated by RANKL, which promotes osteoclast differentiation [23,28]. Studies have shown that RANKL induces ROS production in osteoclastogenesis, which in turn enhances the activation of RANKL-mediated signaling, stimulates bone resorption and exacerbates bone loss, playing an important role in the development of osteoporosis [23]. Several studies have demonstrated that inhibiting ROS production prevents osteoclastogenesis [29–31]. We investigated the effect of Gar C on intracellular oxidative stress during RANKL stimulation and showed that Gar C significantly inhibited intracellular ROS levels. Nrf2 is a core transcription factor that regulates oxidative stress and promotes the expression of downstream antioxidant enzymes [32]. Nrf2 deficiency increases serum RANKL concentrations and promotes osteoclast proliferation [33]. Oxidative stress conditions activate Nrf2 signaling, promote its translocation to the nucleus, and induce the expression of the antioxidant cytoprotective gene HO-1, thereby preventing oxidative damage [34]. In the present study, we demonstrated that Gar C upregulated the ROS scavenger HO-1 to inhibit osteoclast differentiation. RANKL stimulation reduced Nrf2 protein expression and favored ROS signaling, while Gar C treatment restored and dose-dependently increased Nrf2 expression and promoted Nrf2 nuclear translocation, suggesting that Gar C may, at least in part, inhibit intracellular ROS through Nrf2 and other antioxidant enzymes that upregulate intracellular ROS.

Bone remodeling is a tightly coupled process involving both osteoblasts and osteoclasts. These cells are essential for bone remodeling. Osteoclasts, which are the only bone resorbing cells in the body, are multinucleated cells formed by the fusion of osteoclast progenitors from the monocyte/macrophage lineage of the bone marrow, which are produced by hematopoietic stem cells (HSCs) and secrete H+, Cl -, and cathepsin K (CTSK) in the resorption zone in response to M-CSF and RANKL activation. CTSK and matrix metalloproteinases (MMPs) degrade the bone matrix [35]. Osteoclasts adhere to the bone matrix through the dynamic structure of footlets, allowing osteoclasts to move across the bone surface through cytoskeletal reorganization, which mediates bone resorption [36]. Thus, the number and area of osteoclasts attached to the surface of the bone matrix is positively correlated with the ability of these cells to resorb bone. In addition, the secretion of osteoclast-related functional proteins is equally important for bone resorption. In this study, our results show for the first time that Gar C inhibits RANKL-mediated osteoclastogenesis and bone destruction. TRAP staining showed a significant decrease in the number and area of osteoclasts with increasing Gar C concentrations. In addition, immunofluorescence staining showed that Gar C significantly inhibited the formation of actin rings in osteoclasts. The Western blot results showed that Gar C could affect the expression of osteoclast-related functional proteins and transcription factors, which was consistent with previous studies. In conclusion, our results suggest that Gar C has an inhibitory effect on osteoclast formation and activation, resulting in reduced bone resorption in vitro.

Gar C is a naturally occurring xanthone extracted from the fruit and rind of the mangosteen that has a variety of functional biological functions, such as anti-inflammatory, antioxidant and antimicrobial functions [13,37,38]. Studies have shown that daily oral intake of fresh mangosteen juice may prevent estrogen-deficient bone loss [39]. The active ingredient of mangosteen is α-mangiferin, which has been reported to inhibit osteoclasts in animals [40], and α-mangiferin can treat inflammation-related diseases by blocking macrophage activation [41]. α-Mangiferin and Gar C are derivatives of the natural phenolic antioxidant luteolin. α-Mangiferin is a *para*-dihydroxy-substituted derivative of luteolin, while Gar C is a para- and o-dihydroxy-substituted derivative. A study suggests that the antioxidant activity and mechanism are derived from the effectiveness of certain specific substituents in luteolin. The o-position substituent may have a better antioxidant effect [12]. Our results also show that Gar C can effectively inhibit oxidative stress during osteoclast differentiation and inhibit osteoclast activation. The in vivo results confirm that Gar C can inhibit osteoporosis.

NF-κB plays a crucial role in osteoclast differentiation [42]. NF-κB is activated by inflammatory conditions and is a multifunctional group of transcription factors that not only transcriptionally regulate cellular inflammatory responses but also participate in the expression of a variety of genes involved in normal cellular activities. In RANKL knockout mice [43], NF-κB can promote osteoclastogenesis by activating the RANKL/RANK pathway [44]. Blocking NF-κB signaling is thought to be an effective way to prevent osteoclast activity [21,22,45]. Nrf2 is a redox-sensitive transcription factor that controls cellular antioxidant defenses by inducing antioxidant gene expression [46]. Crosstalk between Nrf2 and NF-κB plays a key role in osteoclasts and has recently become the focus of much research [47]. Furthermore, previous studies have shown that RANKL-induced osteoclastogenesis typically involves the activation of both the ROS and NF-κB signaling pathways [48]. ROS can mediate RANKL-induced osteoclast differentiation by inhibiting IKK phosphatase and directly or indirectly regulating activation of the transcription factor NF-κB in osteoclasts [49,50]. Therefore, we explored whether Gar C could inhibit the activation of the NF-κB pathway. In other studies, Garcinone B, a Garcinia analog of Gar C, blocked LPS-induced NF-κB-dependent transcription [51], and Garcinia cambogia extracted from mangosteen downregulated IκBa and NF-κB (p65) in the NFκB pathway [52]. In this study, the results showed that Gar C inhibited the

phosphorylation and degradation of IκBα and P65. In terms of the time-dependent effects of Gar C on the NF-κB pathway, Gar C delayed the time at which phosphorylated P65 (PP65) reached its peak and significantly reduced the rate of phosphorylation and degradation of IκBα.

This study also has some limitations. First, our study demonstrated that Gar C inhibited ROS production, downregulated the NF-κB pathway and suppressed osteoclastogenesis. However, there is growing evidence that ROS production supports various pathological conditions, including inflammation and osteoporosis [53], and that osteoclast activation involves inflammatory factors [54]. Therefore, we should further investigate whether regulated osteoclasts are involved in the anti-inflammatory effects of Gar C. Second, bone metabolism homeostasis involves osteoclast-induced bone resorption and osteoblast-induced bone formation. In the present study, we demonstrated that Gar C inhibited osteoclasts, but the effect of Gar C on osteoblasts is unknown. Work on this topic is currently being carried out by our team.

5. Conclusion

In conclusion, in this study, our results suggest that Gar C significantly reduces OVX-induced osteoporosis by inhibiting osteoclast activation through oxidative stress. This mechanism was associated with inhibition of the NF-κB pathway (Scheme 1). These results further support Gar C as a potential drug candidate for the treatment of osteoporosis.

Funding

We greatly acknowledge the financial support from the National Natural Science Foundation of China (82074473, 82104892, 82305038 and 82305115), the Key Disciplines in Suzhou (SZXK202120, LCZX202221and LCZX202331), the Suzhou Science and Technology Development Plan Project (SYSD2020009, SYSD2021175, SKY2021001, SKJY2021002, KJXW2021066, SKY2023081,

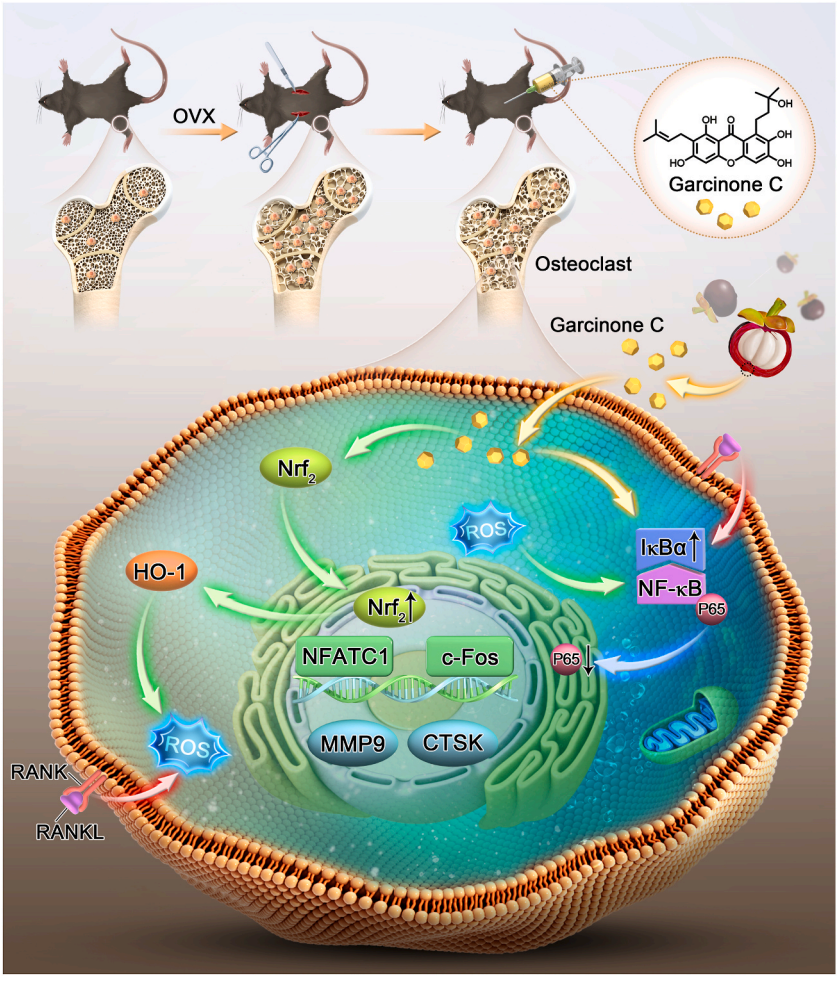

Scheme 1. Garcinone C Attenuates RANKL-Induced Osteoclast Differentiation and Oxidative Stress by Activating Nrf2/HO-1 and Inhibiting the NF-kB Signaling Pathway.

SKY2023079 and SKY2023012), the Zhangjiagang Health Personnel Training Project (ZJGWSRC2020002).

Availability of data

The raw data supporting the conclusions of this paper will be provided by the authors to any qualified researcher without reservation.

Ethical statement

Animal studies were reviewed and approved by the Animal Ethics and Welfare Committee (AEWC) of Zhangjiagang TCM Hospital Affiliated to Nanjing University of Chinese Medicine (Approval NO: AEWC-20220412).

CRediT authorship contribution statement

Hongyun Ji: Formal analysis, Conceptualization. **Qian Pan:** Software, Conceptualization. **Ruihong Cao:** Supervision, Software, Resources. **Yajun Li:** Methodology, Investigation. **Yunshang Yang:** Software, Resources. **Shuangshuang Chen:** Resources, Funding acquisition. **Yong Gu:** Methodology, Formal analysis. **Daoyi Qian:** Project administration, Investigation. **Yang Guo:** Visualization, Validation. **Liangliang Wang:** Visualization, Resources, Project administration. **Zhirong Wang:** Writing – review & editing, Writing – original draft. **Long Xiao:** Writing – review & editing, Writing – original draft, Software, Project administration, Methodology, Funding acquisition.

Declaration of competing interest

The authors declare that the study was conducted in the absence of any business or financial relationships that could be construed as potential conflicts of interest.

Appendix A. Supplementary data

Supplementary data to this article can be found online at https://doi.org/10.1016/j.heliyon.2024.e25601.

References

[1] X. Zhu, W. Bai, H. Zheng, Twelve years of GWAS discoveries for osteoporosis and related traits: advances, challenges and applications, Bone Res 9 (1) (2021) 23.
[2] F. Pouresmaeili, et al., A comprehensive overview on osteoporosis and its risk factors, Therapeut. Clin. Risk Manag. 14 (2018) 2029–2049.
[3] N.E. Lane, Epidemiology, etiology, and diagnosis of osteoporosis, Am. J. Obstet. Gynecol. 194 (2 Suppl) (2006) S3–S11.
[4] S.E. Putnam, et al., Natural products as alternative treatments for metabolic bone disorders and for maintenance of bone health, Phytother Res. 21 (2) (2007) 99–112.
[5] L. Zhang, et al., Exercise for osteoporosis: a literature review of pathology and mechanism, Front. Immunol. 13 (2022) 1005665.
[6] X. Chen, et al., Nrf2 epigenetic derepression induced by running exercise protects against osteoporosis, Bone Res 9 (1) (2021) 15.
[7] T.J. De Vries, et al., M-CSF priming of osteoclast precursors can cause osteoclastogenesis-insensitivity, which can be prevented and overcome on bone, J. Cell. Physiol. 230 (1) (2015) 210–225.
[8] J. William, W.S.S. Boyle, David L. Lacey, Osteoclast Differentiation and Activation, Nature Publishing Group, 2003.
[9] J. Lorenzo, The many ways of osteoclast activation, J. Clin. Invest. 127 (7) (2017) 2530–2532.
[10] H. Tao, et al., ROS signaling cascades: dual regulations for osteoclast and osteoblast, Acta Biochim. Biophys. Sin. 52 (10) (2020) 1055–1062.
[11] A.Y.H. Ng, et al., Regulator of G protein signaling 12 enhances osteoclastogenesis by suppressing Nrf2-dependent antioxidant proteins to promote the generation of reactive oxygen species, Elife 8 (2019).
[12] X. Li, et al., 2-Phenyl-4,4,5,5-tetramethylimidazoline-1-oxyl 3-oxide radical (PTIO*) Trapping activity and mechanisms of 16 phenolic xanthones, Molecules 23 (7) (2018).
[13] X. Yang, et al., Garcinone D, a natural xanthone promotes C17.2 neural stem cell proliferation: Possible involvement of STAT3/Cyclin D1 pathway and Nrf2/HO-1 pathway, Neurosci. Lett. 626 (2016) 6–12.
[14] T.H. Tran, , et al.S.V. Garcinoxanthones, New xanthone derivatives from the pericarps of Garcinia mangostana together with their cytotoxic and antioxidant activities, Fitoterapia 151 (2021) 104880.
[15] M. Abate, et al., Mangostanin, a xanthone derived from Garcinia mangostana fruit, exerts protective and reparative effects on oxidative damage in human keratinocytes, Pharmaceuticals 15 (1) (2022).
[16] L. Yang, Z. Xu, W. Wang, Garcinone-E exhibits anticancer effects in HeLa human cervical carcinoma cells mediated via programmed cell death, cell cycle arrest and suppression of cell migration and invasion, Amb. Express 10 (1) (2020) 126.
[17] X.H. Xu, et al., Garcinone E induces apoptosis and inhibits migration and invasion in ovarian cancer cells, Sci. Rep. 7 (1) (2017) 10718.
[18] Y. Xia, et al., Garcinone C exerts antitumor activity by modulating the expression of ATR/Stat3/4EBP1 in nasopharyngeal carcinoma cells, Oncol. Rep. 39 (3) (2018) 1485–1493.
[19] J. Chen, et al., Garcinone C suppresses colon tumorigenesis through the Gli1-dependent hedgehog signaling pathway, Phytomedicine 79 (2020) 153334.
[20] Y. Zhou, et al., Garcinone C suppresses tumorsphere formation and invasiveness by hedgehog/gli1 signaling in colorectal cancer stem-like cells, J. Agric. Food Chem. 70 (26) (2022) 7941–7952.
[21] Q. Zhuang, et al., Avicularin alleviates osteoporosis in ovariectomized mice by inhibiting osteoclastogenesis through NF-kappaB pathway inhibition, J. Agric. Food Chem. 71 (2023) 411–420.
[22] Y. Li, et al., Urolithin B Suppressed Osteoclast Activation and Reduced Bone Loss of Osteoporosis via Inhibiting ERK/NF-κB Pathway, Cell proliferation, 2022 e13291.

[23] T.S. Agidigbi, C. Kim, Reactive oxygen species in osteoclast differentiation and possible pharmaceutical targets of ROS-mediated osteoclast diseases, Int. J. Mol. Sci. 20 (14) (2019).
[24] M.J. Morgan, Z.G. Liu, Crosstalk of reactive oxygen species and NF-kappaB signaling, Cell Res. 21 (1) (2011) 103–115.
[25] L. Wang, et al., Mechanical regulation of bone remodeling, Bone Res 10 (1) (2022) 16.
[26] S. Song, et al., Advances in pathogenesis and therapeutic strategies for osteoporosis, Pharmacol. Ther. 237 (2022) 108168.
[27] L. Gambari, et al., Sodium hydrosulfide inhibits the differentiation of osteoclast progenitor cells via NRF2-dependent mechanism, Pharmacol. Res. 87 (2014) 99–112.
[28] H. Kanzaki, et al., The Keap1/Nrf2 protein axis plays a role in osteoclast differentiation by regulating intracellular reactive oxygen species signaling, J. Biol. Chem. 288 (32) (2013) 23009–23020.
[29] X. Su, et al., Artesunate attenuates bone erosion in rheumatoid arthritis by suppressing reactive oxygen species via activating p62/Nrf2 signaling, Biomed. Pharmacother. 137 (2021) 111382.
[30] S. Ni, et al., Schisandrin A restrains osteoclastogenesis by inhibiting reactive oxygen species and activating Nrf2 signalling, Cell Prolif. 53 (10) (2020) e12882.
[31] M.Z. Long Xiao, Yu Huang, Jie Zhu, Wenkai Tang, Danyong Li, Jiandong Shi, Aiqing Lu, Huilin Yang, Dechun Geng, Li Hong, Zhirong Wang, Puerarin Alleviates Osteoporosis in the Ovariectomy-Induced Mice by Suppressing Osteoclastogenesis via Inhibition of TRAF6/ROS- Dependent MAPK/NF-κB Signaling Pathways, 2020.
[32] P. Xue, et al., Deficiency of optineurin enhances osteoclast differentiation by attenuating the NRF2-mediated antioxidant response, Exp. Mol. Med. 53 (4) (2021) 667–680.
[33] T. Rana, et al., Loss of Nrf2 accelerates ionizing radiation-induced bone loss by upregulating RANKL, Free Radic. Biol. Med. 53 (12) (2012) 2298–2307.
[34] H.J. Kim, et al., Sargassum serratifolium attenuates RANKL-induced osteoclast differentiation and oxidative stress through inhibition of NF-kappaB and activation of the Nrf2/HO-1 signaling pathway, Biosci Trends 12 (3) (2018) 257–265.
[35] Y. Sun, et al., Recent advances in osteoclast biological behavior, Front. Cell Dev. Biol. 9 (2021) 788680.
[36] D.J. Hadjidakis, Androulakis II, Bone remodeling, Ann. N. Y. Acad. Sci. 1092 (2006) 385–396.
[37] B. Ovalle-Magallanes, D. Eugenio-Perez, J. Pedraza-Chaverri, Medicinal properties of mangosteen (Garcinia mangostana L.): a comprehensive update, Food Chem. Toxicol. 109 (Pt 1) (2017) 102–122.
[38] M.C. Nauman, J.J. Johnson, The purple mangosteen (Garcinia mangostana): defining the anticancer potential of selected xanthones, Pharmacol. Res. 175 (2022) 106032.
[39] C. Vellapandian, et al., A comparative study of actinidia deliciosa and Garcinia mangostana in ovariectomy-induced osteoporosis in female wistar rats, BioMed Res. Int. 2017 (2017) 5349520.
[40] W. Zhang, et al., α-Mangostin inhibits LPS-induced bone resorption by restricting osteoclastogenesis via NF-κB and MAPK signaling, Chin. Med. 17 (1) (2022) 34.
[41] S. Tewtrakul, C. Wattanapiromsakul, W. Mahabusarakam, Effects of compounds from Garcinia mangostana on inflammatory mediators in RAW264.7 macrophage cells, J. Ethnopharmacol. 121 (3) (2009) 379–382.
[42] W. Tang, et al., Puerarin inhibits titanium particle-induced osteolysis and RANKL-induced osteoclastogenesis via suppression of the NF-kappaB signaling pathway, J. Cell Mol. Med. 24 (20) (2020) 11972–11983.
[43] B.F. Boyce, Z. Yao, L. Xing, Functions of nuclear factor kappaB in bone, Ann. N. Y. Acad. Sci. 1192 (2010) 367–375.
[44] Z.H. Lee, H.H. Kim, Signal transduction by receptor activator of nuclear factor kappa B in osteoclasts, Biochem. Biophys. Res. Commun. 305 (2) (2003) 211–214.
[45] Z. Ping, et al., Inhibitory effects of melatonin on titanium particle-induced inflammatory bone resorption and osteoclastogenesis via suppression of NF-kappaB signaling, Acta Biomater. 62 (2017) 362–371.
[46] J. Li, et al., Paeonol attenuates ligation-induced periodontitis in rats by inhibiting osteoclastogenesis via regulating Nrf2/NF-kappaB/NFATc1 signaling pathway, Biochimie 156 (2019) 129–137.
[47] J.D. Wardyn, A.H. Ponsford, C.M. Sanderson, Dissecting molecular cross-talk between Nrf2 and NF-kappaB response pathways, Biochem. Soc. Trans. 43 (4) (2015) 621–626.
[48] H.S. Kim, et al., DJ-1 controls bone homeostasis through the regulation of osteoclast differentiation, Nat. Commun. 8 (1) (2017) 1519.
[49] D.A. Callaway, J.X. Jiang, Reactive oxygen species and oxidative stress in osteoclastogenesis, skeletal aging and bone diseases, J. Bone Miner. Metabol. 33 (4) (2015) 359–370.
[50] H. Blaser, et al., TNF and ROS crosstalk in inflammation, Trends Cell Biol. 26 (4) (2016) 249–261.
[51] T. Yamakuni, et al., Garcinone B reduces prostaglandin E2 release and NF-kappaB-mediated transcription in C6 rat glioma cells, Neurosci. Lett. 394 (3) (2006) 206–210.
[52] H.S. Chae, et al., Mangosteen extract prevents dextran sulfate sodium-induced colitis in mice by suppressing NF-kappaB activation and inflammation, J. Med. Food 20 (8) (2017) 727–733.
[53] Y. Xian, et al., Oroxylin A reduces osteoclast formation and bone resorption via suppressing RANKL-induced ROS and NFATc1 activation, Biochem. Pharmacol. 193 (2021) 114761.
[54] Y.H. Hwang, et al., The natural product 6-gingerol inhibits inflammation-associated osteoclast differentiation via reduction of prostaglandin E(2) levels, Int. J. Mol. Sci. 19 (7) (2018).